AMERICAN SOCIETY FOR MICROBIOLOGY | Infection and Immunity

Murine Model for Preclinical Studies of Var2CSA-Mediated Pathology Associated with Malaria in Pregnancy

Luciana V. de Moraes,[a] Sebastien Dechavanne,[b,c,d,e] Patrícia M. Sousa,[a] André Barateiro,[a] Sónia F. Cunha,[a] Sofia Nunes-Silva,[b,c,d,e] Flávia A. Lima,[f] Oscar Murillo,[f] Claudio R. F. Marinho,[f] Stephane Gangnard,[b,c,d,e] Anand Srivastava,[b,c,d,e] Joanna A. Braks,[g] Chris J. Janse,[g] Benoit Gamain,[b,c,d,e] Blandine Franke-Fayard,[g] Carlos Penha-Gonçalves[a]

Instituto Gulbenkian de Ciência, Oeiras, Portugal[a]; Inserm UMR_1134, Paris, France[b]; Université Paris Diderot, Sorbonne Paris Cité, UMR_S1134, Paris, France[c]; Institut National de la Transfusion Sanguine, Paris, France[d]; Laboratory of Excellence GR-Ex, Paris, France[e]; Departamento de Parasitologia, Universidade de São Paulo-ICB/USP, São Paulo, SP, Brazil[f]; Leiden Malaria Research Group, Department of Parasitology, Leiden University Medical Center, Leiden, The Netherlands[g]

Plasmodium falciparum **infection during pregnancy leads to abortions, stillbirth, low birth weight, and maternal mortality. Infected erythrocytes (IEs) accumulate in the placenta by adhering to chondroitin sulfate A (CSA) via var2CSA protein exposed on the *P. falciparum* IE membrane. *Plasmodium berghei* IE infection in pregnant BALB/c mice is a model for severe placental malaria (PM). Here, we describe a transgenic *P. berghei* parasite expressing the full-length var2CSA extracellular region (domains DBL1X to DBL6ε) fused to a *P. berghei* exported protein (EMAP1) and characterize a var2CSA-based mouse model of PM. BALB/c mice were infected at midgestation with different doses of *P. berghei*-var2CSA (*P. berghei*-VAR) or *P. berghei* wild-type IEs. Infection with 10^4 *P. berghei*-VAR IEs induced a higher incidence of stillbirth and lower fetal weight than *P. berghei*. At doses of 10^5 and 10^6 IEs, *P. berghei*-VAR-infected mice showed increased maternal mortality during pregnancy and fetal loss, respectively. Parasite loads in infected placentas were similar between parasite lines despite differences in maternal outcomes. Fetal weight loss normalized for parasitemia was higher in *P. berghei*-VAR-infected mice than in *P. berghei*-infected mice. *In vitro* assays showed that higher numbers of *P. berghei*-VAR IEs than *P. berghei* IEs adhered to placental tissue. Immunization of mice with *P. berghei*-VAR elicited IgG antibodies reactive to DBL1-6 recombinant protein, indicating that the topology of immunogenic epitopes is maintained between DBL1-6–EMAP1 on *P. berghei*-VAR and recombinant DBL1-6 (recDBL1-6). Our data suggested that impairments in pregnancy caused by *P. berghei*-VAR infection were attributable to var2CSA expression. This model provides a tool for preclinical evaluation of protection against PM induced by approaches that target var2CSA.**

Malaria is a major health concern in countries where it is endemic. Recent reports show an incidence of 198 million cases in 2013 (82% in Africa) and 584,000 estimated deaths, 74% of which were children under 5 years of age (1). In areas of endemicity, pregnant women are under a greater risk of malaria than nonpregnant (NP) women due to immunological and hormonal changes and higher attractiveness to mosquitoes (2). Placental infection or clinical malaria during pregnancy has been shown to have a negative impact on infant health, increasing the risk of clinical malaria and mortality in infants (3).

In areas of unstable malaria transmission, pregnant women can develop severe malaria due to low immunity to the parasite, which has been associated with increased mortality during pregnancy (4, 5), miscarriages, preterm deliveries, low birth weight, stillbirth, and death of neonates (6). These features can be recapitulated in a mouse model of severe placental malaria (PM) (7), which consists of infection of BALB/c mice syngeneically pregnant with parasites of the ANKA strain of the rodent malaria parasite *Plasmodium berghei*.

Apart from physiological changes associated with gestation, increased susceptibility to developing malaria during pregnancy is attributed to the placenta as a preferred site of accumulation of infected erythrocytes (IEs). The placenta offers a niche for IE sequestration due to its microcirculatory properties (8) and to the expression of chondroitin sulfate A (CSA), an essential receptor for the *Plasmodium falciparum* var2CSA variant antigen expressed on the surface membranes of IEs (9–11). Physical interaction between var2CSA and CSA allows adhesion of IEs to placental tissue (11, 12). Sequestration of IEs in the placenta is thought to be a critical factor in pathogenesis associated with PM (13, 14). Although *P. berghei* lacks proteins that have homology to var2CSA, *P. berghei* IEs have been shown to bind to the placenta in a CSA-dependent manner (7, 15). We have recently shown *in vivo* that sequestration of *P. berghei* IEs in pregnant BALB/c mice is facilitated in areas of low maternal blood flow in the placenta (8), suggesting an important role for placental microcirculation in the process.

var2CSA is a large (~350-kDa) polymorphic protein exported to the surface of the IE and a variant antigen of the *P. falciparum* erythrocyte membrane protein 1 (PfEMP1) family encoded by the *var* genes (16). The extracellular region is composed of six different Duffy binding-like (DBL) domains and interdomain regions (DBL1X to DBL6ε [DBL1-6]) and is transcriptionally upregulated in CSA-binding parasites (10). Var2CSA is so far the best-charac-

Received 22 September 2015 **Returned for modification** 31 October 2015
Accepted 23 March 2016

Accepted manuscript posted online 4 April 2016

Citation de Moraes LV, Dechavanne S, Sousa PM, Barateiro A, Cunha SF, Nunes-Silva S, Lima FA, Murillo O, Marinho CRF, Gangnard S, Srivastava A, Braks JA, Janse CJ, Gamain B, Franke-Fayard B, Penha-Gonçalves C. 2016. Murine model for preclinical studies of Var2CSA-mediated pathology associated with malaria in pregnancy. Infect Immun 84:1761–1774. doi:10.1128/IAI.01207-15.

Editor: J. H. Adams, University of South Florida

Address correspondence to Luciana V. de Moraes, lmoraes@igc.gulbenkian.pt, or Blandine Franke-Fayard, B.Franke-Fayard@lumc.nl.

terized molecule involved in cytoadhesion in the placenta (9, 17). High levels of anti-var2CSA antibodies have been detected in pregnant women from areas where *P. falciparum* is endemic (9) and have been associated with improved pregnancy outcomes (9, 18). These observations strongly suggest var2CSA as a strong target for vaccines aiming at preventing pathology associated with PM.

Here, we describe a transgenic *P. berghei* parasite expressing the full-length extracellular region of the var2CSA PfEMP1 (DBL1-6) (*P. berghei*-VAR) and develop a novel var2CSA-based mouse model of PM by infecting allogeneically pregnant BALB/c mice at midgestation with *P. berghei*-VAR. The extracellular region of var2CSA is fused to the exported protein EMAP1 (erythrocyte membrane-associated protein 1) of *P. berghei* that is localized at the surface membrane of *P. berghei* IEs (19). We found that PM pathology is more severe in mice infected with *P. berghei*-VAR than in mice infected with wild-type *P. berghei*. We also show that anti-DBL1-6 antibodies recognize *P. berghei* proteins, suggesting epitope sharing between var2CSA and *P. berghei* surface proteins. IgG antibodies generated by immunization with *P. berghei*-VAR IEs recognized full-length DBL1-6 recombinant protein (recDBL1-6) (20). This model provides an experimental system for studying interaction of var2CSA with CSA, for investigating the dynamics of *P. berghei*-VAR accumulation in the placenta, and for preclinical evaluation of PM vaccine candidates targeting the var2CSA antigen.

MATERIALS AND METHODS

Ethics statement. All procedures involving laboratory mice were in accordance with national (Portaria 1005/92) and European (European Directive 86/609/CEE) regulations on animal experimentation and were approved by the Instituto Gulbenkian de Ciência ethics committee and the Direcção-Geral de Veterinária (the official national entity for regulation of laboratory animal use).

Animals and pregnancy monitoring. Eight- to 12-week-old female BALB/c mice were obtained from our animal facility at Instituto Gulbenkian de Ciência. The mice were bred and maintained under specific-pathogen-free (SPF) conditions.

Allogeneic pregnancy model. Two BALB/c females were transferred to a cage with one C57BL/6 male and removed after detection of vaginal plugs; the day of removal was considered gestational day 1 (G1). The females were weighed immediately after they were separated from the males and on G13; a gain of approximately 5 g of body weight during this period was indicative of pregnancy. This breeding type generates a high number of offspring with small variation in weight.

Parasites. The *P. berghei* ANKA reporter line 1037cl1 (ANKA-GFP-Lucschiz [Luc]; mutant RMgm-32) (http://www.pberghei.eu), which contains the *gfp-luc* fusion gene under the control of the schizont-specific *ama1* promoter integrated into the silent 230p gene locus (PBANKA_0306000) and does not contain a drug-selectable marker (21), was used to obtain *P. berghei*-VAR. *P. berghei* ANKA-GFP-Luc (1037cl1) parasites (*P. berghei*) were also used in all experiments.

Generation of *P. berghei* parasites expressing var2CSA. A transgenic 1037cl1 strain that expresses C-terminally *var2csa*-tagged EMAP1 (gene model PBANKA_0836800; *emap1*::*var2csa*; line 1653cl3) was generated as previously reported for C-terminally mCherry-tagged EMAP1 (19). The synthetic 3D7-DBL1X-6ε gene (*var2csa*; PF3D7_1200600) (20) was first subcloned into PCR2.1 Topo (Invitrogen, Netherlands), and the C-terminal region of *emap1* from pL1534 (BamHI/SpeI) was N-terminally fused to the 3D7-DBL1X-6ε gene (NdeI/SpeI). The PCR-amplified 3′ untranslated region (UTR) of the calmodulin (*cam*) gene (PBANKA_1010600) was then cloned as an XbaI fragment downstream of the *emap1*:3D7-DBL1X-6ε fusion using the following primer set: 5397, 5′ ATCTAGATAAT TATTAATATATATGAATATATATACATCGTTG, and 5398, 5′ ATCTAG AGGTACCGACCATATAAGAATTAAC. Finally, after the destruction of NdeI, the KpnI fragment containing the *emap1*::3D7-DBL1X-6ε–3′ UTR *cam* was cloned into pL0007 to create pL1593. The final DNA construct was linearized with NdeI before transfection. Transfection, selection, and cloning of transformed parasites were performed using standard genetic-modification technologies for *P. berghei* (22), using *P. berghei* (1037cl1) as the parental parasite line. Cloned parasite lines were obtained (exp. 1653; transfection of pL1593 into strain 1037cl1) by the method of limiting dilution. Correct integration of DNA constructs and disruption of genes were verified by Southern analyses of pulsed-field gel (PFG)-separated chromosomes (22). PFG-separated chromosomes were hybridized with the 3′ UTR of the *P. berghei dhfr/ts* gene recognizing the endogenous *dhfr/ts* locus on chromosome 7, the green fluorescent protein (GFP)-Lucschiz expression cassette on chromosome 3, and the integrated locus at chromosome 8.

Northern blotting. Transcription of *emap1*::*var2csa* was determined by Northern analysis of RNA samples obtained from *P. berghei* and *P. berghei*-VAR parasite blood stages from asynchronous *in vivo* infections. Northern blots were hybridized with a 3′ fragment of *emap1* PCR amplified from genomic wild-type *P. berghei* (ANKA) using primer pair 3800 (5′ GCCGGTACCGTTGCCATTAGTATGAAGAAATAG) and 3001 (5′ GCCAAGCTTGTTGTGGTCATCTATATCTACTGATG).

Western blotting. *P. berghei* and *P. berghei*-VAR IEs from Nycodenz (Lucron Bioproducts, Belgium)-purified schizonts were collected from overnight cultures (5 μl) (22). Total protein extracts were incubated for 10 min at 70°C with sample-reducing agent and loading buffer (Life Technologies). After migration in an SDS-PAGE gel, 4 to 12% proteins were transferred to polyvinylidene difluoride (PVDF) membranes (Life Technologies). Expression of DBL1-6 fused to EMAP1 was detected by incubation with purified polyclonal rabbit IgG anti-DBL1-6 antibody (23) diluted to 0.1 μg/ml in blocking buffer, followed by incubation with horseradish peroxidase (HRP)-conjugated goat anti-rabbit IgG secondary antibody (Invitrogen). Immunostained protein complexes were visualized by enhanced chemiluminescence (Amersham).

Detection of var2CSA protein by immunofluorescence. var2CSA expression was analyzed with anti-DBL1-6 rabbit polyclonal antibodies (20). Live parasites were collected in phosphate-buffered saline (PBS) or complete RPMI 1640 culture medium and were examined by microscopy using a Leica DMR fluorescence microscope with standard UV GFP and Texas Red filters. Parasite nuclei were labeled by staining with Hoechst-33258 (Sigma, Netherlands). To detect var2CSA exposed on the surfaces of live parasites, the parasites were first incubated with rabbit anti-DBL1-6 antibody at room temperature for 30 min. After a wash with 500 μl of RPMI 1640 medium (400 × *g*; 2 min), the parasites were stained with Alexa Fluor 594-labeled donkey anti-rabbit (Invitrogen, Netherlands; 1:500) at room temperature (RT) for 30 min. Finally, the parasite nuclei were labeled by staining with Hoechst-33258 (2 μmol/liter; Sigma, Netherlands), and red blood cell surface membranes were stained with the anti-mouse TER-119-fluorescein isothiocyanate (FITC) antibody (1:200; eBioscience, Netherlands) at RT for 30 min and washed with 500 μl of RPMI 1640 medium (400 × *g*; 2 min).

Experiment design. Infected erythrocyte preparations were obtained from one *in vivo* passage in BALB/c mice when the percentage of infection reached approximately 3 to 5%. Parasitemia was measured by flow cytometry to detect DRAQ5 (BioStatus Limited, United Kingdom)-labeled parasites as described previously (24). Pregnant mice were infected intravenously with 10^6, 10^5, or 10^4 IEs at G13 and weighed daily; parasitemia was evaluated from day 3 postinfection until the termination of pregnancy. Nonpregnant mice were infected the same day as pregnant females, and parasitemia was monitored accordingly. Pregnancy outcomes were assessed.

Pregnancy outcomes. Litter size, newborn weight and viability, abortions, and maternal mortality were recorded. Maternal weight was controlled daily from day 3 postinfection. Weight gain was calculated by subtracting the weight on the previous day divided by the number of

fetuses. The birth of dead fetuses and mummified forms attached to the placenta were considered stillbirths. Fetuses that had been expelled before the termination of gestation were recorded as aborted. Abortions were considered loss of the entire litter. Nonaborted fetuses were killed by combining hypothermia and CO_2 narcosis.

Synchronization of parasites. *P. berghei* and *P. berghei*-VAR IEs were cultured to generate synchronized mature schizonts as previously described (22). Briefly, IEs from frozen stock were injected into nonpregnant BALB/c mice. When parasitemia reached 10%, IEs were injected into naive nonpregnant BALB/c mice (1 passage). Mice were bled when parasitemia reached 1 to 3%. Red blood cells were resuspended in RPMI containing 20% fetal bovine serum (FBS) and 0.1% neomycin and incubated for 18 h in 75-cm^2 tissue culture flasks in a total volume of 50 ml. Schizont-stage IEs were isolated using magnetically activated cell sorting (MACS) 25LS columns (Miltenyi Biotec) according to the manufacturer's instructions. For cytoadherence assays IEs were synchronized in neomycin-free medium for 12 h.

***Ex vivo* cytoadherence assays.** Placentas from noninfected BALB/c females, obtained at G19, were treated using a previously described protocol (25). Briefly, the placentas were fixed in 2% formalin and 0.5% glutaraldehyde for 10 min and heated in a microwave oven before being embedded in paraffin. After being deparaffinized and rehydrated, 5-μm sections were delimited with a hydrophobic circle using a PAP pen (Sigma-Aldrich). The sections were blocked with 1% bovine serum albumin (BSA) in PBS at RT for 30 min. Fifty microliters of synchronized IE suspension (schizont stage), at a concentration of 10^8/ml, was added to the tissue sections for 60 min at 37°C in a humid chamber. After washing unbound cells, placental sections were stained with Giemsa for 8 min. For IE-ligand-blocking experiments, synchronized IEs were preincubated with doses (10 to 1,000 μg/ml) of CSA from bovine tracheas (Sigma) at 37°C for 30 min without agitation. As a negative control, IEs were treated with trypsin (2.5 mg/ml; Gibco) for IE-ligand cleavage. The IEs were then added to the placental sections as described above. The slides were mounted with Tissue-Tek glass mounting medium (Sakura) and examined on a Zeiss Axio Image M2 microscope (magnification, ×1,000). The number of IEs adhering to placental sections under each experimental condition was determined in a blind fashion by counting 10 fields. The data were expressed as the average number of IEs per 1.5 mm^2 of placental tissue. Images were obtained with an AxioCam HRc digital camera using AxioVision software.

Flow cytometry. IEs purified by MACS were incubated with anti-CD16/CD32 (Fc block) for 10 min, followed by incubation with purified rabbit anti-DBL1-6 IgG (23) and TER 119-phycoerythrin (PE) (Molecular Probes, USA) for 30 min on ice. Cells were washed in PBS containing 2% fetal calf serum (FCS) and 0.01% sodium azide (fluorescence-activated cell sorter [FACS] buffer), incubated with anti-rabbit IgG-A647 (Jackson Immuno Research Laboratories), washed twice with FACS buffer, and analyzed in a FACSCalibur (BD Biosciences) after acquisition of 100,000 events.

Evaluation of antibody titers by enzyme-linked immunosorbent assay (ELISA). Mice were infected with 10^6 *P. berghei*-VAR or *P. berghei* IEs and treated intraperitoneally (i.p.) with 3 consecutive doses of chloroquine (0.7 mg) when peripheral parasitemia reached 10%. The mice were reinfected with the same dose and parasite line 30 days later. Sera were collected 45 days after reinfection by cardiac puncture. High-binding 96-well plates (Nunc, Thermo Scientific) were coated with 0.1 μg/ml of recombinant DBL1-6 protein (recDBL1-6) (20) in PBS and incubated overnight. The wells were washed 3 times with PBS-Tween 20 (0.05%) (PBS-T) and blocked with PBS-T–4% BSA for 1 h at 37°C. Serially diluted serum was incubated for 1 h at 37°C. After 3 washes, the wells were incubated with horseradish peroxidase-conjugated rat anti-mouse IgG Fcγ-specific antibody (Jackson ImmunoResearch Laboratories) for 1 h at 37°C. The reaction was developed with TMB (BD Biosciences) and interrupted with 2N H_2SO_4; plates were read at 450 nm.

Parasite quantification in placentas. Total RNA from individual *P. berghei*- or *P. berghei*-VAR-infected placentas was obtained using an RNeasy minikit (Qiagen) according to the manufacturer's instructions for animal tissues. Total RNA (500 ng) was converted to cDNA (Transcriptor First Strand cDNA synthesis kit; Roche) using random-hexamer primers. cDNA specific to *P. berghei* 18S rRNA was amplified with TaqMan specific primers: forward, 5′-CCG ATA ACG AAC GAG ATC TTA ACC T-3′; reverse, 5′-CGT CAA AAC CAA TCT CCC AAT AAA GG-3′; probe, 5′-ACT CGC CGC TAA TTA G-3′ (FAM/MGB) (24). Endogenous control glyceraldehyde-3-phosphate dehydrogenase (GAPDH) (Mouse GAPD endogenous control; Applied Biosystems) was used in multiplex PCRs (ABI Prism 7900HT; Applied Biosystems). Cycle threshold (C_T) values of the target gene were subtracted by C_T values of the endogenous control (ΔC_T); results are expressed as $\log(2^{-\Delta CT})$.

Statistical analysis. Data are displayed as scattered dot plots with lines at the mean (normal distribution) or median (nonnormal distribution) or are depicted in box-and-whiskers plots (nonnormally distributed). Unpaired *t* tests, Mann-Whitney tests, analysis of variance (ANOVA) with Bonferroni's correction for multiple-comparison tests or Kruskal-Wallis with Dunn's multiple-comparison tests, Spearman correlation, and nonlinear regression (one-phase exponential decay) were performed using GraphPad Prism 4.0 software. Multiple linear regression was performed using R. Multiple-comparison tests were performed on selected pairs of columns for proper adjustments of the *P* value. Observed differences were considered statistically significant for *P* values of <0.05; the level of significance cutoff was properly adjusted when applicable.

RESULTS

Generation and characterization of transgenic *P. berghei*-VAR parasites. To construct a mouse model closer to the pathogenesis of human PM, we sought tools to present the *P. falciparum* CSA-binding extracellular var2CSA region on the surfaces of IEs. Recently, we applied a combination of proteomic, genomic, and reverse-genetic approaches to identify proteins that are exported into the cytoplasm of infected erythrocytes of the rodent model parasite *P. berghei* (19). Two exported proteins that are transported to the IE surface were identified and were named EMAPs. EMAP1 (PBANKA_0836800) is a member of the PEXEL-negative *P. berghei* multigene family fam-a, and EMAP2 (PBANKA_0316800) is a PEXEL-positive protein encoded by a single-copy gene; neither protein plays a direct role in sequestration. In this study, we generated a transgenic parasite line in which a synthetic 3D7-DBL1X-6ε gene (*var2csa*; PF3D7_1200600) is fused C terminally to the *emap1* gene. Tagging of *emap1* was performed by standard genetic modification technologies in which the *emap1* endogenous gene is stably tagged with *var2csa* by a single-crossover integration of the tagging construct (Fig. 1A and B). Transfection of wild-type *P. berghei* and drug selection followed by cloning of transfected parasites resulted in the selection of the transgenic parasite line *P. berghei*-VAR. Genotyping by Southern analysis of PFG-separated chromosomes of *P. berghei*-VAR confirmed that the *emap1*::*var2csa*-construct (pL1593) was correctly integrated into the *emap1* locus (Fig. 1C). Northern and Western blot analyses were performed to analyze the expression level of *emap1*::*var2csa* in IEs. The level of *emap1*::*var2csa* transcripts in *P. berghei*-VAR is similar to the level of *emap1* transcript in *P. berghei* parasites (Fig. 1C). Detection of the EMAP1::var2CSA protein was performed by Western blot analysis using rabbit anti-DBL1-6 polyclonal antibodies (23). Bands with a molecular mass of ≥250 kDa were detected in *P. berghei*-VAR, comparable to the size of var2CSA expressed by *P. falciparum* (16) and likely to be monomers and dimers of var2CSA (Fig. 1D). The

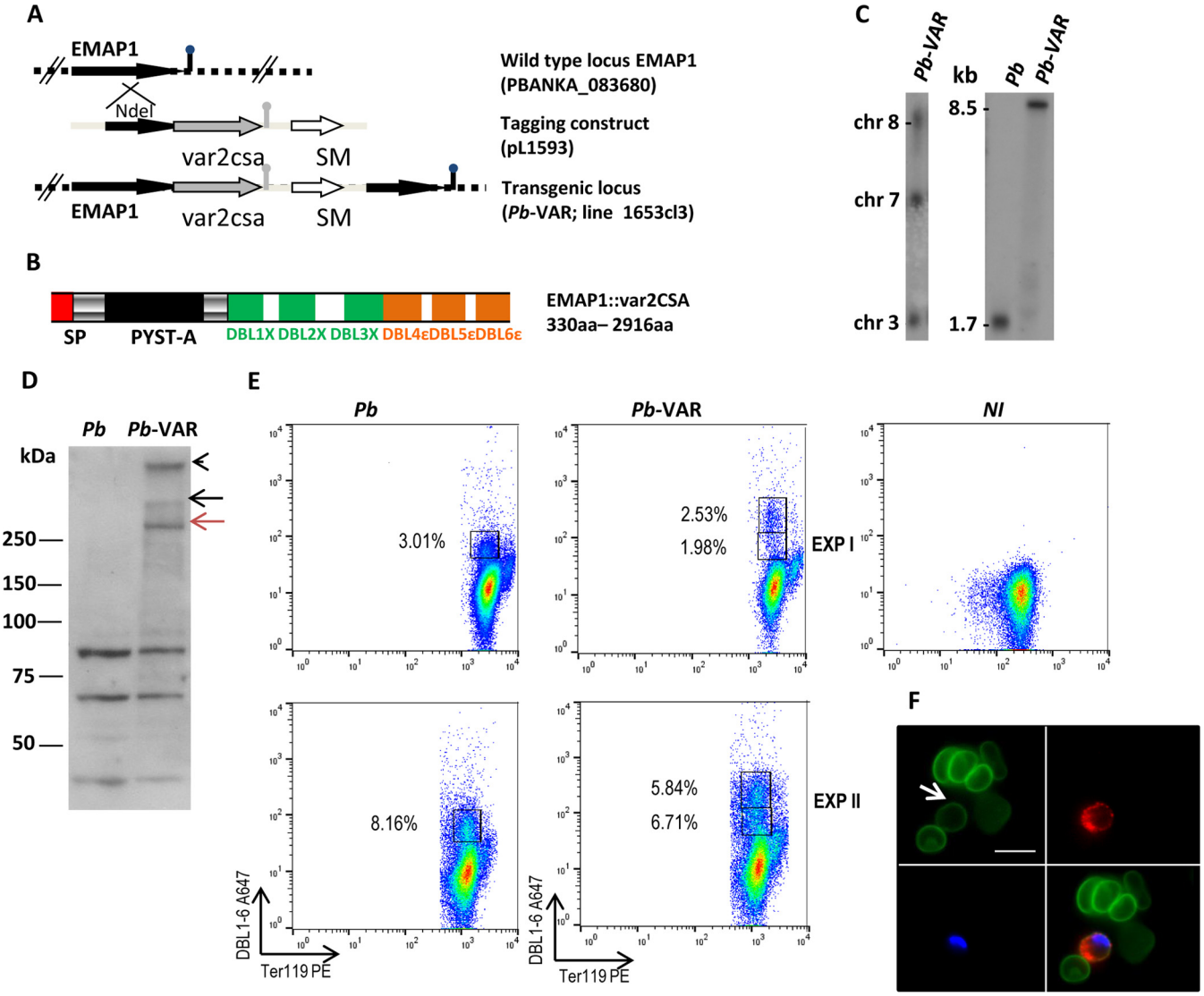

FIG 1 Generation, genotyping, and expression of EMAP1::var2CSA in transgenic *P. berghei*-VAR. (A) Schematic representation of the wild-type *emap1* locus before and after integration of the construct (pL1593) used to generate the transgenic line (1653cl3) expressing EMAP1 that is C-terminally tagged with the *var2csa* synthetic gene (3D7-DBL1X-6ε [cf. panel B]). The construct (middle) contains the *hdhfr* selectable marker cassette (SM) (white arrow) and the C-terminal region of the *emap1* gene for integration (black arrow) in the endogenous gene (top) by single-crossover homologous recombination. (B) Schematic of the EMAP1 protein tagged with the synthetic 3D7-DBL1X-6ε region of var2CSA showing the locations of a predicted signal peptide (SP) and the *Plasmodium yoelii* subtelomeric A (PYST-A) domain of EMAP fused to the 6 DBL domains of var2CSA. (C) (Left) Diagnostic Southern analysis of pulsed-field gel-separated chromosomes (chr) confirmed the correct tagging of *emap1* in *P. berghei* (*Pb*)-VAR parasites. Separated chromosomes were hybridized with the 3′ UTR of *P. berghei dhfr/ts* recognizing the tagged *emap1* locus at chromosome 8, in addition to the endogenous *dhfr/ts* gene on chromosome 7 and the GFP-luciferase reporter integrated into chromosome 3 of the parent wild-type line. (Right) Northern blot analysis demonstrating expression of the *var2csa*-tagged version of *emap1*. RNA of mixed blood stages was hybridized with a PCR probe recognizing the 3′ end of the *emap1* gene (primers 3800/3001) detecting an 8.5-kb transcript. (D) Western blotting of Nycodenz-purified schizont lysates from *P. berghei* and *P. berghei*-VAR parasites; the var2CSA protein was detected using primary rabbit anti-var2CSA IgG polyclonal antibodies, followed by anti-rabbit IgG HRP-conjugated secondary antibody. The black and red arrows indicate a dimer and a monomer of var2CSA, respectively; the arrowhead indicates the bottom of the well of the gel or var2CSA multimers. (E) Scatter plots (2 independent experiments [EXP]) of synchronized MACS-purified IEs containing schizonts from *P. berghei*- or *P. berghei*-VAR-infected nonpregnant mice and noninfected erythrocytes (NI) stained with anti-DBL1-6-Alexa-fluor- and anti-TER 119-PE antibodies. (F) Immunofluorescence assay of live *P. berghei*-VAR schizont-containing IEs showing DBL1-6-positive (red) (upper right) and -negative (green) (upper left) IEs. Erythrocyte membranes were stained with TER 119 (green) and DNA with Hoechst (blue) (lower left): lower right, merged images. The arrow points to a DBL1-6^{+} IE. Scale bar, 10 μm.

protein was not detected in *P. berghei* IE extracts, although anti-DBL1-6 antibodies recognized smaller proteins in both *P. berghei* and *P. berghei*-VAR parasites (Fig. 1D). In line with the Western blot analysis, FACS data show DBL1-6 reactivity in a fraction of MACS-purified *P. berghei* and *P. berghei*-VAR IEs containing schizonts but not in noninfected erythrocytes (Fig. 1E). Nevertheless, it is clear that the *P. berghei*-VAR IEs contain a population with higher DBL1-6 reactivity, which is not present among *P. berghei* IEs that presumably correspond to the var2CSA-expressing erythrocytes comprising 2.5% to 5.8% of IEs (Fig. 1E). DBL1-6 staining

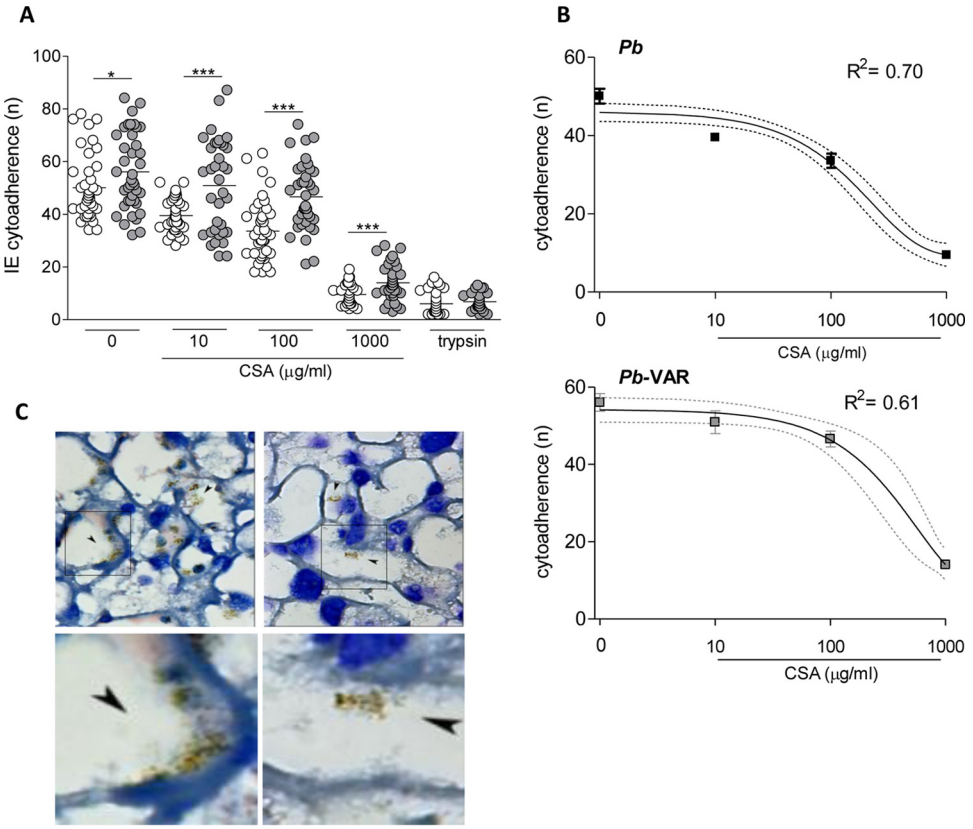

FIG 2 *P. berghei*-VAR and *P. berghei* IEs bind to placental sections in a CSA-dependent manner. (A) *P. berghei*-VAR and *P. berghei* IEs pretreated or not with different concentrations of CSA were added to placental sections for 30 min; after various washes, the remaining IEs in 10 fields of the tissue section were counted. The results are expressed as the number of bound IEs (*n*) per 1.5 mm^2 of area of placental tissue; *, $P < 0.05$; ***, $P < 0.001$ (unpaired *t* test). (B) One-phase exponential decay for cytoadherence of *P. berghei* and *P. berghei*-VAR IEs according to CSA concentration. The error bars indicate standard errors, and the dotted line indicates the 95% confidence interval. (C) (Upper left and upper right) Representative images of Giemsa-stained labyrinthine regions of placentas incubated with untreated *P. berghei*-VAR IEs (upper left) or with *P. berghei*-VAR IEs that were pretreated with CSA (1,000 μg/ml) (upper right); the arrowheads indicate IEs that are recognized by clusters of hemozoin pigment (brown). (Lower left and lower right) Images enlarged from the boxed areas in the upper left and upper right images, respectively. Magnification of upper panels, ×1,000.

of live *P. berghei*-VAR IEs was also confirmed by fluorescence microscopy (Fig. 1F). Taken together, these results indicate that the var2CSA region of EMAP1::var2CSA is exposed on the membrane in a fraction of *P. berghei*-VAR IEs. The observation that anti-DBL1-6 antibodies reacted to *P. berghei* IEs but not to noninfected erythrocytes suggests that molecules expressed on the surfaces of *P. berghei* IEs may share epitope homology with DBL domains.

More *P. berghei*-VAR IEs than *P. berghei* IEs bind to placental tissue. Next, we compared the capacities of *P. berghei*-VAR and *P. berghei* IEs to bind to the mouse placenta *in vitro*. *P. berghei* IEs have been previously shown to bind to mouse placentas in a CSA-dependent manner (7). *P. berghei* or *P. berghei*-VAR IE suspensions (at the schizont stage) were preincubated with or without different concentrations of CSA (10 to 1,000 μg/ml) and were subsequently added to thin sections of placental tissue. Under all tested conditions, the number of *P. berghei*-VAR IEs that adhered to the tissue was significantly higher than that of *P. berghei* IEs (Fig. 2A). Multiple linear regression including the parasite line and CSA concentration showed an adjusted R^2 value of 0.64 and an *F* statistic of 185.6 (data not shown). This model indicates that *P. berghei*-VAR has higher cytoadherence than *P. berghei* ($P < 0.01$) and that cytoadherence decreases with the CSA concentration ($P < 0.01$). Multiple linear regression showed that dependency on interaction with placental CSA is marginally higher in *P. berghei*-VAR IEs than in *P. berghei* IEs ($P = 0.09$; data not shown), possibly due to the low number of *P. berghei*-VAR IEs expressing var2CSA, which is also suggested by linear regression analysis (Fig. 2B).

***P. berghei*-VAR infection elicits an anti-DBL1-6 specific antibody response.** RecDBL1-6 is a candidate molecule for a vaccine against PM to reduce pathogenesis. It has been shown to be correctly folded, and immunization with recDBL1-6 resulted in the generation of specific IgG responses in small animals (23). We assessed whether infection with *P. berghei*-VAR could elicit antibodies that recognized recDBL1-6 and if *P. berghei* non-var2CSA proteins would cross-react with recDBL1-6. Mice were infected with *P. berghei*-VAR or *P. berghei* IEs, treated with chloroquine, and reinfected with the same parasite line 30 days later. Sera were collected 45 days after reinfection, and IgG responses against recDBL1-6 were evaluated by ELISA (Fig. 3). *P. berghei*-VAR-infected mice showed high anti-DBL1-6 IgG titers. Although *P. berghei* IE infection generated IgG antibodies reactive to recDBL1-6, titers were significantly lower than *P. berghei*-VAR-induced responses. The observation that IgG antibodies from sera of mice immunized with *P. berghei*-VAR recognize recDBL1-6 is indica-

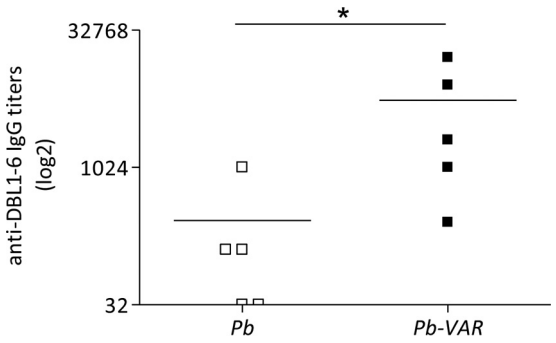

FIG 3 Higher levels of anti-var2CSA antibodies are induced by infection with *P. berghei*-VAR than by *P. berghei* infection. Sera were collected from mice that were repeatedly infected with *P. berghei*-VAR or *P. berghei* IEs and cured with chloroquine. Anti-var2CSA IgG antibody titers were determined by ELISA using 0.1 μg/ml of recDBL1-6 coating; *, $P < 0.05$ (Mann-Whitney test). Note that sera from *P. berghei*-infected mice also recognized recDBL1-6.

tive that DBL1-6-EMAP1 maintains the topology of immunogenic epitopes on recDBL1-6. Recognition of recDBL1-6 by IgG from sera of *P. berghei*-infected mice, although at a significantly lower level, is in agreement with Western blot and FACS analyses showing reactivity of *P. berghei* IEs with anti-DBL1-6 antibodies. The fact that bands reactive to anti-DBL1-6 antibodies in *P. berghei* and *P. berghei*-VAR IEs have the same molecular weight does not imply they share common immunogenic epitopes. Nevertheless, we cannot exclude the hypothesis of cross-reactivity between *P. berghei* and DBL1-6 proteins.

IE expansion in maternal blood during pregnancy. We next tested the ability of *P. berghei*-VAR parasites to induce PM and the impact of infection on pregnancy outcomes compared to infections with *P. berghei*. Allogeneically pregnant BALB/c mice (BALB/c × C57BL/6 mating) were infected at G13 with different IE doses (10^4, 10^5, and 10^6 IEs). Maternal parasitemia was assessed daily from day 3 postinfection by measuring IEs in tail blood. The area under the parasitemia curve (AUC) was used as a proxy for blood parasite mass during the infection period in order to compare parasite expansion in *P. berghei*- and *P. berghei*-VAR-infected mice. Susceptibility to infection, as determined by parasite expansion in peripheral blood, was increased in pregnant (P) mice compared to nonpregnant (NP) females, irrespective of the infection dose and parasite line (P *P. berghei* versus NP *P. berghei* at 10^6 IEs, $P < 0.01$; P *P. berghei*-VAR versus NP *P. berghei-VAR* at all doses, $P < 0.001$; P *P. berghei* versus NP *P. berghei* at 10^5 and 10^4 IEs, $P < 0.001$) (Fig. 4A to C). As expected, parasitemia in pregnant and nonpregnant mice increased according to the IE dose in both *P. berghei* and *P. berghei*-VAR infections (Fig. 4D and E). Injection of 10^4 *P. berghei*-VAR IEs led to an increase in parasitemia levels at day 6 postinfection compared to *P. berghei* injection and an increase in the AUC compared to *P. berghei*, although it was not statistically significant in pregnant mice (Fig. 4A); at higher doses, curves between the two parasite lines were similar in pregnant and nonpregnant mice. These observations indicate that *P. berghei*-

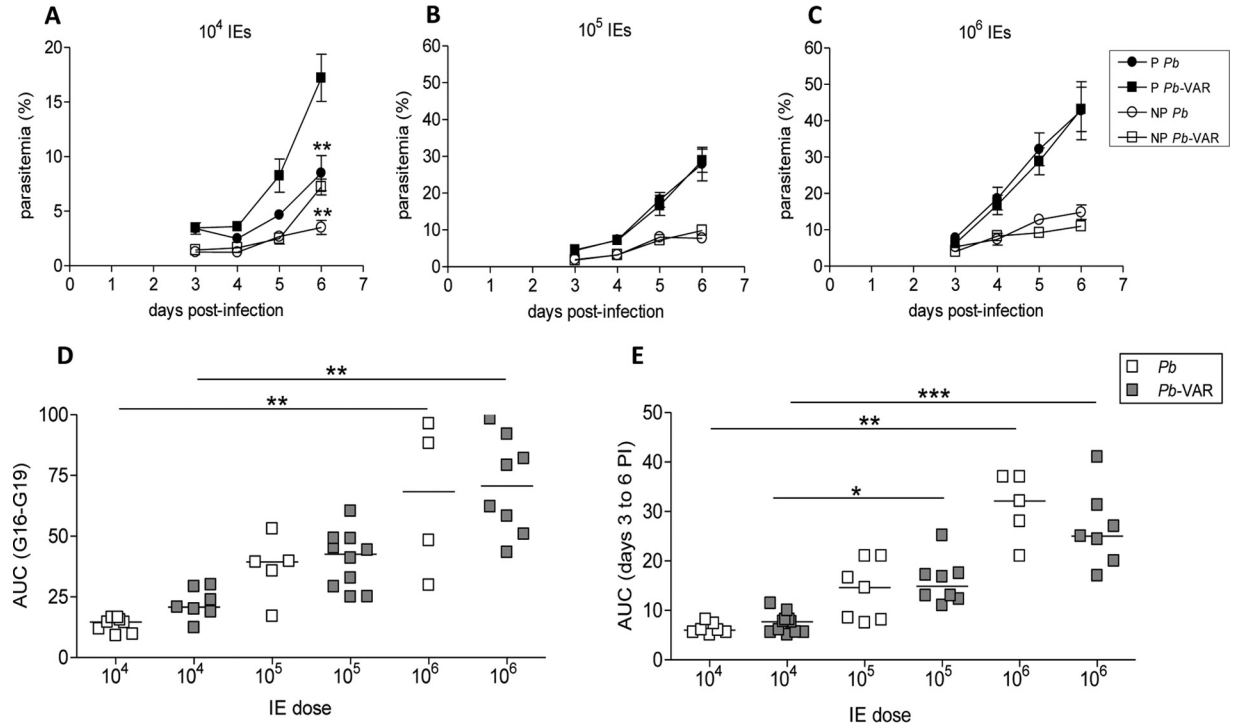

FIG 4 Parasite expansion in peripheral blood. (A to C) BALB/c pregnant (P) mice were infected with 10^4 (A), 10^5 (B), or 10^6 (C) *P. berghei* or *P. berghei*-VAR IEs on G13; nonpregnant (NP) mice were infected on the same day. Parasitemia was evaluated in the peripheral blood from the third day postinfection until delivery, and the AUC during this time was calculated. The error bars indicate standard deviations. **, $P < 0.01$ in comparison with *P. berghei*-VAR (Mann-Whitney test). (D and E) Comparisons of AUCs between *P. berghei* and *P. berghei*-VAR expansion in pregnant mice (D) or nonpregnant females (E). Group sizes: P *P. berghei* (10^6, $n = 8$; 10^5, $n = 5$; 10^4, $n = 8$); P *P. berghei*-VAR (10^6, $n = 7$; 10^5, $n = 7$; 10^4, $n = 7$); NP *P. berghei* (10^6, $n = 6$; 10^5, $n = 7$; 10^4, $n = 7$); NP *P. berghei*-VAR (10^6, $n = 10$; 10^5, $n = 8$; 10^4, $n = 6$). *, $P < 0.05$; **, $P < 0.01$; ***, $P < 0.001$ (Kruskal-Wallis with Dunn's multicomparison test). PI, postinfection.

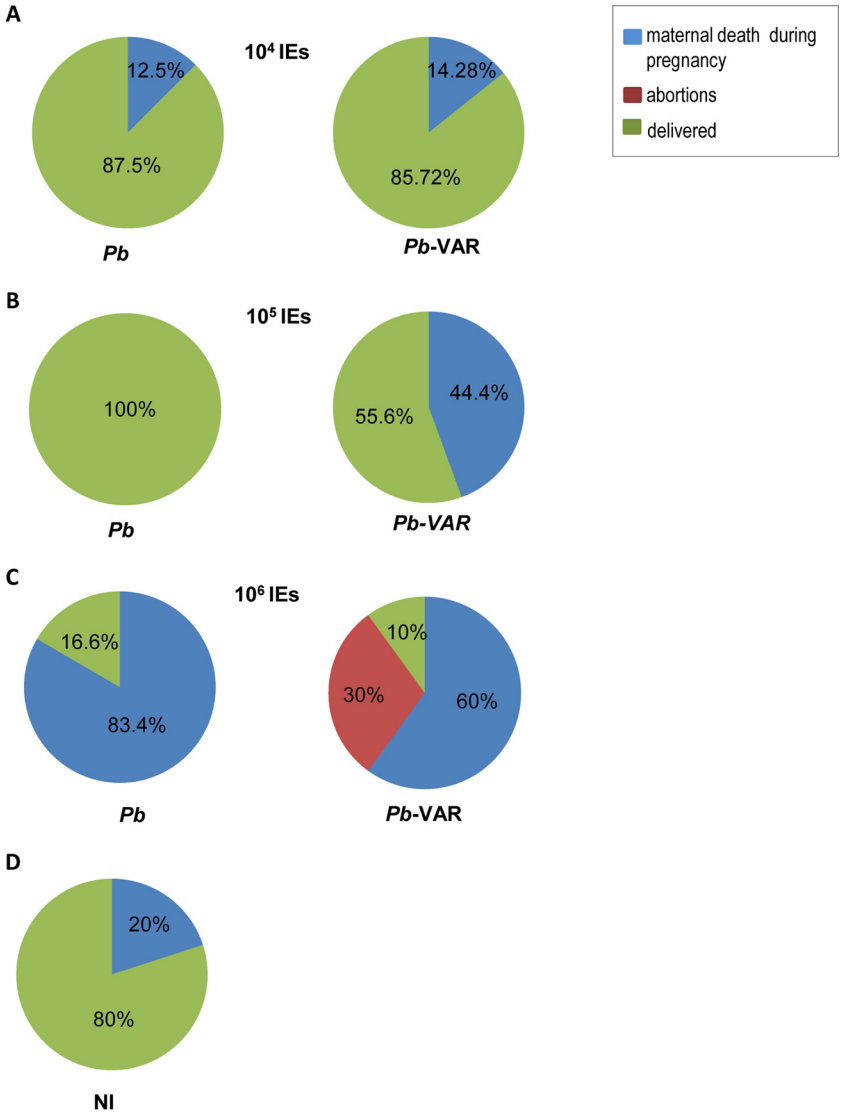

FIG 5 *P. berghei*-VAR infection induces a higher incidence of maternal death before delivery and of abortions than *P. berghei* infection. BALB/c mice were infected with 10^4 (A), 10^5 (B), or 10^6 (C) *P. berghei* or *P. berghei*-VAR IEs on G13 or were not infected (D). Pregnant mice were scored for abortions (considered loss of the entire litter) and maternal mortality until the end of pregnancy (before delivery or at delivery). The percentages refer to the maternal population; *P. berghei* (10^6, $n = 6$; 10^5, $n = 5$), *P. berghei*-VAR (10^6, $n = 10$; 10^5, $n = 9$); noninfected (NI) ($n = 10$).

VAR dynamics at higher IE doses are similar to those of *P. berghei* but that at the lowest dose peripheral *P. berghei*-VAR expansion was observed to be more pronounced in pregnant mice.

Pregnancy outcomes after infection. Pregnancy outcomes, such as newborn weight and viability, abortions, and maternal mortality, were recorded in mice infected with *P. berghei*-VAR and *P. berghei* IEs. At the lowest infection dose (10^4 IEs), apart from 13 to 14% that died during pregnancy, all the mice reached the end of gestation, delivered (Fig. 5A), and survived for at least 7 days postdelivery (data not shown), irrespective of the parasite line. At an infection dose of 10^5 IEs, maternal death during pregnancy occurred in 45% of *P. berghei*-VAR-infected mice with marginal statistical significance compared to *P. berghei* infection (all mice delivered) ($P = 0.078$; chi-square test) (Fig. 5B). At an infection dose of 10^5 IEs, maternal death during pregnancy occurred in 45% of *P. berghei*-VAR-infected mice, showing a trend toward statistical significance compared to *P. berghei* infection (all mice delivered) ($P = 0.078$; chi-square test) (Fig. 5B). No difference was observed in survival after delivery, and maternal death occurred 24 to 48 h after delivery (median survival time for *P. berghei* and *P. berghei*-VAR, 8 days after infection). Infection with 10^6 IEs induced a severe phenotype with high incidence of maternal death before delivery in both the *P. berghei* and *P. berghei*-VAR models and abortion of the entire litter in 30% of *P. berghei*-VAR-infected mice (Fig. 5C). Occasionally, maternal death during pregnancy occurred in noninfected mice (Fig. 5D), but infections with 10^6 IEs in both *P. berghei*- and *P. berghei*-VAR-induced PM showed a clear incremental effect on maternal death ($P = 0.013$ and $P = 0.067$ for *P. berghei* and *P. berghei*-VAR, respectively; chi-square test). In comparison to other doses (10^5 and 10^4 IEs for both parasite lines), no significant associations between infection and maternal death were found ($P = 0.26$; chi-square test). We also

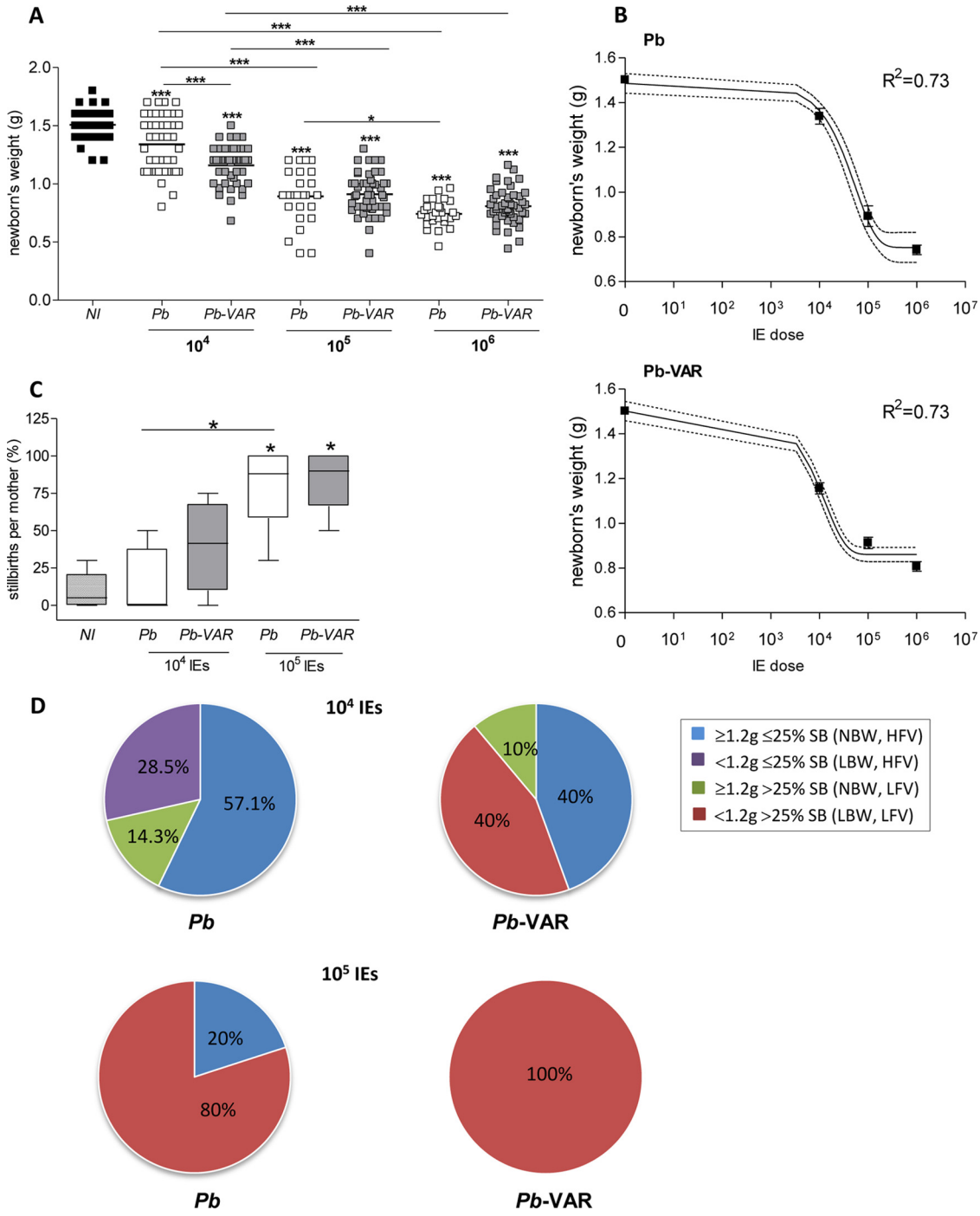

FIG 6 The degree of success of fetal outcomes improves with a lower IE dose. (A) Weights of newborns and fetuses from mothers that died at the end of gestation after infection with different IE doses. (B) One-phase exponential decay of weights of newborns and fetuses from mothers that died before delivery according to IE dose for *P. berghei* and *P. berghei*-VAR. (C) Percentages of stillbirths per mother after injection of different doses of *P. berghei* (white) or *P. berghei*-VAR (gray) IEs. (D) Pregnancy outcomes as determined by the combination of birth weight and incidence of stillbirths per mother. Numbers of pregnant mice: *P. berghei* (10^5, $n = 5$; 10^4, $n = 7$); *P. berghei*-VAR (10^5, $n = 5$; 10^4: $n = 5$). *, $P < 0.05$; ***, $P < 0.001$ (asterisks over symbols [A] or boxes [C] represent comparisons to noninfected mice, and asterisks over horizontal lines represent comparisons between the indicated groups). (A) ANOVA with Bonferroni's multicomparison test. (B) The error bars indicate standard errors, and the dotted line indicates the 95% confidence interval. (C) Kruskal-Wallis with Dunn's multicomparison test. The horizontal lines indicate means.

observed a dose effect on fetal outcomes for both *P. berghei* and *P. berghei*-VAR: there was a decrease in birth weight (Fig. 6A and B) and an increase in stillbirths (intrauterine fetal death) (Fig. 6C). Interestingly, infection with 10^4 IEs in both PM models induced significant reduction of birth weight in *P. berghei*-VAR compared to *P. berghei* infections (Fig. 6A); moreover, compared to *P. berghei*-induced outcomes, infection with 10^4 *P. berghei*-VAR IEs was more severe: we observed a clear trend toward a higher incidence

TABLE 1 Associations between low fetal viability and low birth weight in pregnant mice infected with *P. berghei*-VAR IEs[a]

Birth wt (no. of pregnancies)	Fetal viability (no. of pregnancies)	
	Low (≤25%)	High (>25%)
Normal (≥1.2 g)	2	1
Low (<1.2 g)	0	8

[a] Association between phenotypes: $P = 0.01$ (chi-square test).

TABLE 2 Associations between low fetal viability and low birth weight in pregnant mice infected with *P. berghei* IEs[a]

Birth wt (no. of pregnancies)	Fetal viability (no. of pregnancies)	
	Low (≤25%)	High (>25%)
Normal (≥1.2 g)	6	1
Low (<1.2 g)	2	3

[a] Association between phenotypes: $P = 0.097$ (chi-square test).

of stillbirths and lower birth weight, whereas for other doses (10^5 and 10^6 IEs), no differences in these parameters were observed between *P. berghei*- and *P. berghei*-VAR-infected mice (Fig. 6C and D). Multiple linear regression including the IE dose and parasite line was also applied and showed an adjusted R^2 of 0.36 and an *F* statistic of 44.3 (data not shown). This analysis indicates that weight decreases with IE dose ($P < 0.01$) and that in the case of infections with *P. berghei*-VAR, the weight decrease is slower than in *P. berghei* infections ($P < 0.01$); this is in line with the one-phase exponential-decay analysis of newborn weight according to the IE dose performed for *P. berghei* and *P. berghei*-VAR infections (Fig. 6B) (*P. berghei*, $K = 1.14e{-}005$ to $2.5e{-}005$; *P. berghei*-VAR, $K = 5.9e{-}005$ to $9.48e{-}005$). Together, the data show that in the *P. berghei*-VAR PM model, a pathogenic role of var2CSA in the fetal outcome (weight loss and stillbirth) is revealed at lower infection doses. Nevertheless, at higher IE doses, var2CSA has a detectable impact on maternal mortality and pregnancy loss (abortion of an entire litter).

Low birth weight is associated with low fetal viability in mice infected with *P. berghei*-VAR. We evaluated fetal outcomes by classifying each litter of infected pregnant mice according to combinations of high (HFV; <25% stillbirths) or low (LFV; >25% stillbirths) fetal viability and averages of normal (NBW; ≥1.2 g) or low (LBW; <1.2 g) birth weight in both 10^5 and 10^4 *P. berghei*-VAR and *P. berghei* infection doses. These splitting values were based on the outcomes for noninfected pregnant females ($n = 6$): the splitting value for birth weight was the lowest weight observed in the litter; the splitting value for stillbirth referred to the highest incidence observed. Comparisons between PM models showed that infection with 10^5 IEs induced the worst fetal outcomes (LFV and LBW) in 100% of *P. berghei*-VAR- and 80% of *P. berghei*-infected mice; infection with 10^4 IEs had no impact on fetal weight and viability (NBW and HFV) in 57% of *P. berghei*- and 40% of *P. berghei*-VAR-infected pregnant mice. However, *P. berghei*-VAR infection still generated severe pathology (LFV and LBW) in 40% of pregnant mice, an effect absent in *P. berghei* infections (Fig. 6E). We observed an association between birth weight and fetal viability in both *P. berghei*-VAR and *P. berghei* infections (Tables 1 and 2, respectively) that was statistically significant only in the former, suggesting that in severe cases, infection compromises both fetal survival and fetal development, an effect that was more pronounced in *P. berghei*-VAR infections.

Parasitemia correlates with birth weight, maternal weight loss, and mortality. The maternal weights of *P. berghei*- and *P. berghei*-VAR-infected and noninfected mice were evaluated for 3 consecutive days starting on day 3 postinfection (G16). The infection dose had a clear effect on the kinetics of weight gain and loss during gestation (Fig. 7), which was more pronounced when mice were infected with 10^6 *P. berghei*-VAR IEs than when mice were infected with other doses (Fig. 7A to C). In this case, weight loss already occurred during the first time window (G16-G17), whereas infections with 10^4 *P. berghei*-VAR IEs induced weight loss at late gestation (G18-G19) (Fig. 7C). In both PM models, parasitemia was negatively correlated with maternal weight gain (Fig. 7D and E) and with birth weight (Fig. 8A and B) and positively correlated with maternal death (Fig. 7F). To ascertain whether differences in pregnancy outcomes in *P. berghei* versus *P. berghei*-VAR infections are due to differences in parasitemia dynamics, we performed an analysis normalizing for parasitemia levels at G19. Fetal weight loss (calculated as the difference from the average weight of newborns from noninfected mothers) was divided by maternal parasitemia values (Fig. 8C to E). Normalized fetal weight loss was increased in *P. berghei*-VAR infections compared to *P. berghei* in infections with 10^4 IEs (Fig. 8C), but not at higher doses (Fig. 8D and E). Normalization to the AUC also showed similar results (10^4 IEs, $P = 0.0002$; 10^5 IEs, $P = 0,43$; 10^6 IEs, $P = 0.05$; unpaired *t* test) (data not shown). These results suggest that aggravated fetal weight loss induced by *P. berghei*-VAR is not due to differences in maternal parasitemia levels but is attributable to var2CSA. Placentas from mice infected with 10^5 *P. berghei* or *P. berghei*-VAR IEs were analyzed for rRNA (18S) *P. berghei* quantification. Parasite loads were not different between *P. berghei*- and *P. berghei*-VAR-infected placentas. These data reinforce the notion that increased maternal (Fig. 5B) and fetal (Fig. 6D) pathology mediated by *P. berghei*-VAR infection is not due to parasite dynamics but to the expression of var2CSA. Taken together, these data strongly suggest that the magnitude of the parasite burden governs different outcomes but increased PM severity induced by *P. berghei*-VAR infection is afforded by var2CSA virulence.

DISCUSSION

In this study, we describe a transgenic *P. berghei* strain that expresses var2CSA and characterize a novel PM model using *P. berghei*-VAR. The extracellular region of var2CSA on the *P. falciparum* IE membrane comprises six DBL domains and a CIDRpam module arranged in the configuration DBL1X-DBL2X-CIDRpam-DBL3X-DBL4ε-DBL5ε-DBL6ε, followed by a single transmembrane helix and a cytoplasmic acidic terminal sequence. In soluble form (no specific orientation), this protein binds specifically and with high affinity to CSA. Furthermore, it has to be noted that the var2CSA protein folded upon itself (20) indicates that DBL1 and DBL6 are close to each other and therefore close to the IE membrane (26), which reinforces the relevance of our construct. Due to the anchoring using the EMAP1 protein, the extracellular region of var2CSA on the surfaces of *P. berghei* erythrocytes was expressed in a mirror orientation: DBL6ε-DBL5ε-DBL4ε-DBL3X-CIDRpam-DBL2X-DBL1X. We provide evidence that DBL1-6 protein is expressed in *P. berghei*-VAR, but only a proportion of IEs containing schizonts exposed the protein on the outer membrane, as revealed by staining live IEs using anti-DBL1-6 antibod-

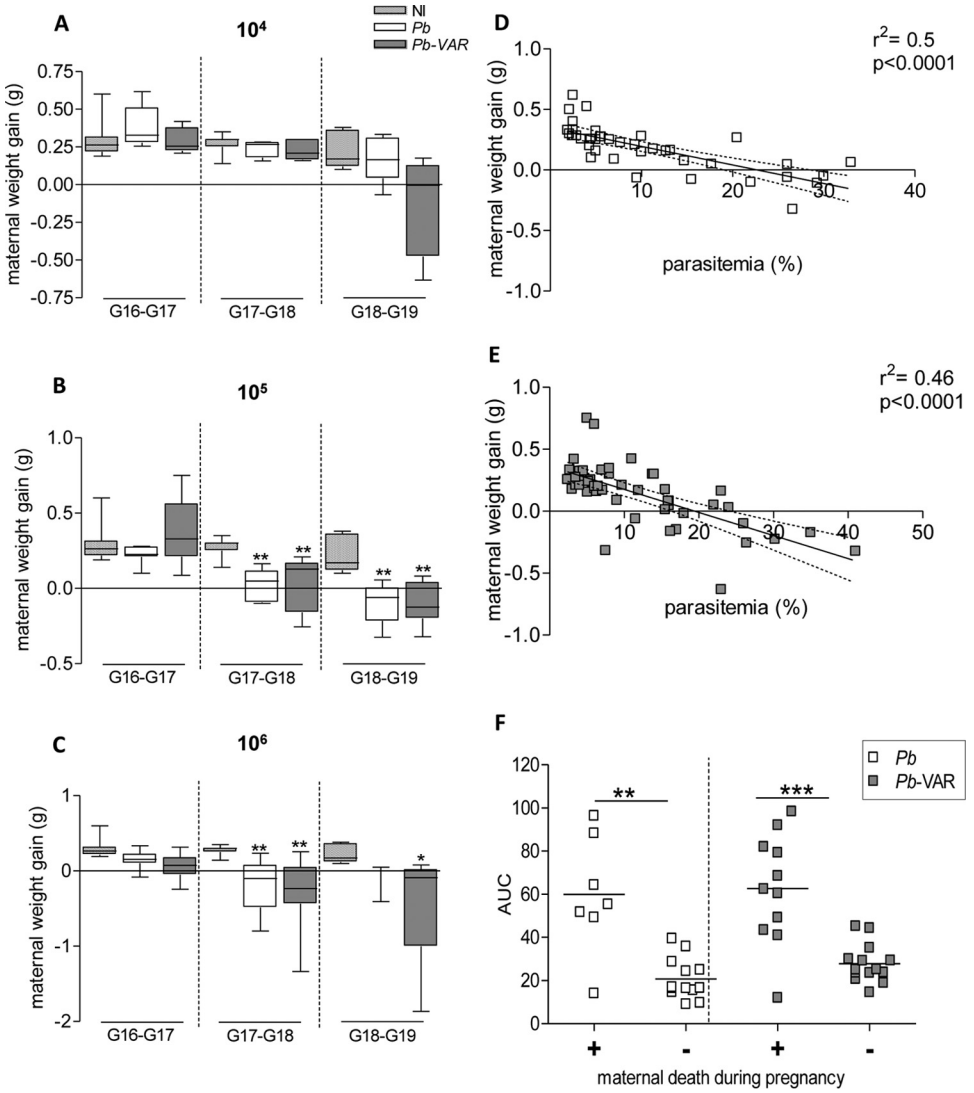

FIG 7 Maternal weight gain correlates with parasitemia in both *P. berghei*-VAR- and *P. berghei*-infected mice. (A to C) Daily maternal weight gain (normalized by the number of fetuses) from G16 until G19 in *P. berghei*- or *P. berghei*-VAR-infected mice with different IE doses. (D and E) Scatterplots displaying pairwise data points of parasitemia and maternal weight gain across G16 to G19 revealing negative correlation in *P. berghei* (D)- and *P. berghei*-VAR (E)-infected mice. The dotted line indicates the 95% confidence interval. (F) Parasitemia (AUC) of mice that died before delivery (+) or that delivered (−) (each square represents one mother). (B and C) *, $P < 0.05$, and **, $P < 0.01$ in comparison to noninfected mice (Kruskal-Wallis with Dunn's multicomparison test). (F) The horizontal lines indicate medians; **, $P < 0.01$; ***, $P < 0.001$ (Mann-Whitney test).

ies. Our data also indicate that surface DBL1-6 maintains recDBL1-6 conformation and enhances binding of IEs to placental tissue *in vitro*.

The outcomes of infection were evaluated in an allogeneic pregnancy model. There are two major reasons for this choice: (i) generation of heterozygosity as a common feature between the mouse model and the human population, since inbreeding is not likely to occur in humans, and (ii) the fact that this breeding type generates high numbers of offspring with small variation in weight, which makes it more appropriate for measuring pregnancy outcomes.

P. berghei-VAR infection generated more severe pregnancy outcomes than in *P. berghei*-infected pregnant mice. Infection with 10^4 *P. berghei*-VAR IEs significantly reduced birth weight, increased the number of stillbirths, and generated higher parasitemia in pregnant mice than *P. berghei* infection. Moreover, pregnancy outcomes in 40% of the mothers infected with 10^4 *P. berghei*-VAR IEs showed the most severe outcomes (a combination of low birth weight [average, <1.2 g] and a high incidence of stillbirths [>30%]), which were not observed in *P. berghei* infection. When mice were infected with higher doses of IEs (10^5 or 10^6 IEs), no significant differences were observed for most of these features, although *P. berghei*-VAR-infected pregnant mice delivered higher numbers of underweight and nonviable neonates than *P. berghei*-infected mice. The incidences of abortions and maternal mortality before delivery were also increased after infection with 10^6 and 10^5 *P. berghei*-VAR IEs, respectively, compared to *P. berghei* infection. A potential explanation for the lack of maternal mortality in infections with 10^5 *P. berghei* IEs (the only group in which this was not observed) and the presence of this feature in noninfected mothers (although rare) could represent an occasional sampling deviation. From our long experience with this

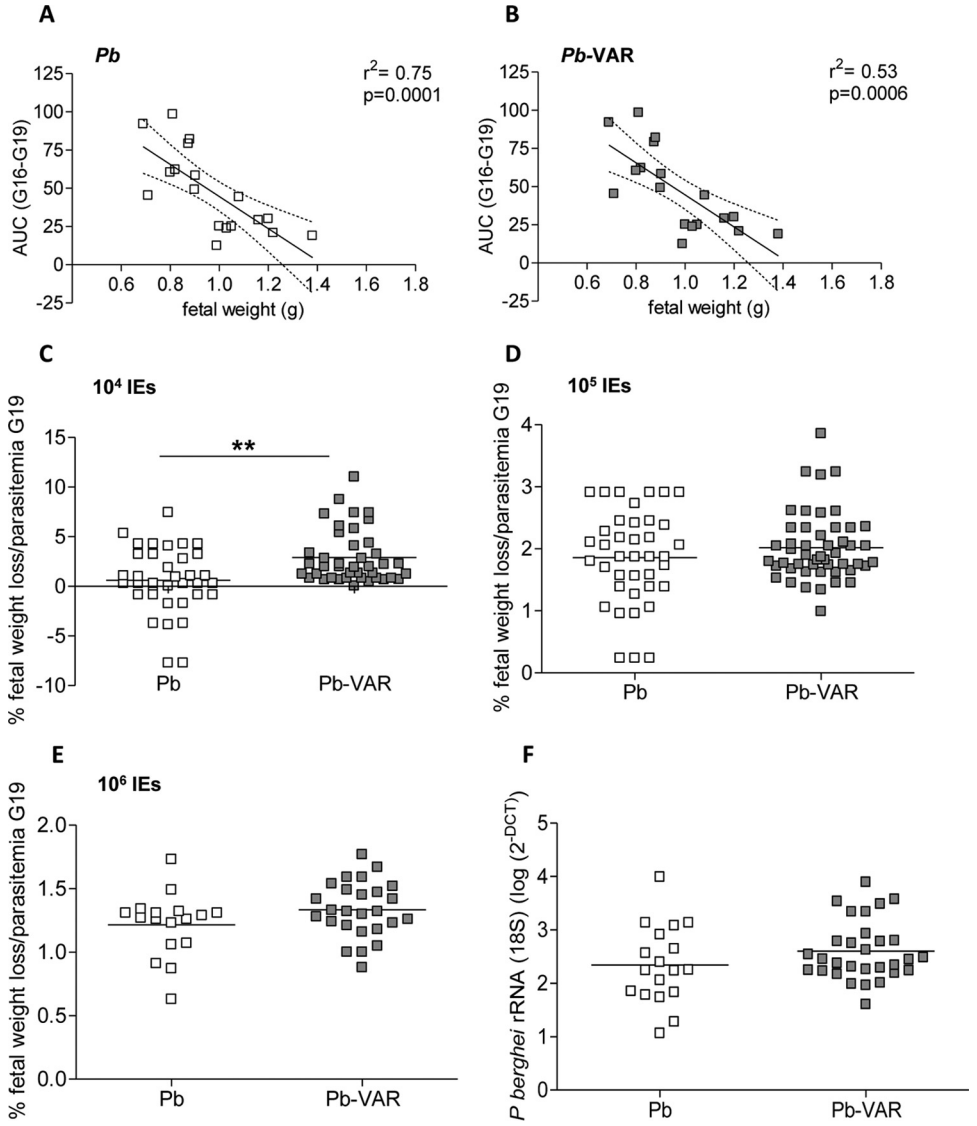

FIG 8 Fetal weight and stillbirth correlate with maternal parasitemia in both *P. berghei*-VAR- and *P. berghei*-infected mice. (A and B) Scatterplots displaying linear regression between the AUC and the average weight of the newborns from the same litter in *P. berghei* (A)- and *P. berghei*-VAR (B)-infected mice. The dotted line indicates the 95% confidence interval. (C to E) Weight loss of fetuses or newborns from *P. berghei*- and *P. berghei*-VAR-infected mice normalized by the percentage of parasitemia at G19. (F) *P. berghei* rRNA (18S) accumulation (quantified as log $2^{-\Delta\Delta CT}$) in placentas of mice infected with *P. berghei* and *P. berghei*-VAR IEs. (C to F) The horizontal lines indicate means; **, $P < 0.01$ (unpaired *t* test).

model, we expect that in a larger group of animals the incidence of maternal mortality would increase in infections with 10^5 *P. berghei* IEs, as well as with *P. berghei*-VAR, rendering the differences between the parasite lines and between infected and noninfected mice more consistent. The cause of death in noninfected mothers was not investigated and could be related to a pregnancy-specific event (such as preeclampsia or hypertension), but unsuccessful pregnancy is not uncommon in laboratory mice.

Our observations demonstrate that expression of var2CSA in *P. berghei* can aggravate pathogenesis, possibly by an increase in the adherence of IEs in the placenta. The less clear differences in pathogenesis between *P. berghei*-VAR and *P. berghei* at higher doses might possibly be due to the strong increase in severe pregnancy outcomes, not only in *P. berghei*-VAR- but also in *P. berghei*-infected mice, thereby hampering the quantification of the possible effects of expression of var2CSA. Nevertheless, we cannot exclude the possibility that a transgenic parasite has a modified virulence that is independent of DBL1-6 expression. Not only pregnancy outcomes, but also the parasite burden in peripheral blood was dependent on the IE dose, and parasitemia was negatively correlated with fetal weight and maternal death before delivery. Maternal death during pregnancy was associated with high parasitemia levels (AUC > 40) after infection with 10^6 IEs but not other doses. At a dose of 10^5 IEs, death during pregnancy was observed only in *P. berghei*-VAR hosts despite a lack of differences in parasitemia levels between *P. berghei* and *P. berghei*-VAR infections. Moreover, we could speculate that the low incidence of maternal mortality after infection with 10^4 *P. berghei*-VAR IEs could be due to significantly reduced proliferation in a period of 6 or 7 days (G13 until the end of pregnancy) compared to the other

doses. Nevertheless, infection with the lowest dose of *P. berghei*-VAR had a more pronounced effect on birth weight and fetal survival, which could be a consequence of higher IE proliferation (possibly due to increased IE binding in the placenta) and host response to var2CSA-CSA interaction.

Mortality in pregnant women with severe malaria has been reported in areas of unstable transmission due to low immunity to the parasite (6). *P. falciparum* malaria was one of the leading causes of death in pregnant women in Thailand; early detection of infection and treatment of malaria significantly reduced mortality in this population (4, 5). Our data suggest that the severity of pregnancy outcomes in the mouse models is highly associated with maternal parasitemia, which in turn probably reflects the level of IE sequestration in the placenta.

Based on our observations, we speculate that aggravation of PM pathology in the *P. berghei*-VAR model is associated at least partially with interactions with trophoblasts rather than with an increased parasite burden. This is supported by our *in vivo* and *in vitro* data. When differences in maternal parasitemia between *P. berghei* and *P. berghei*-VAR in infections with 10^4 IEs were taken into account, *P. berghei*-VAR showed increased severity in maternal and fetal outcomes. We also show that infection at 10^5 *P. berghei*-VAR IEs induced a higher degree of maternal mortality despite similar placental parasite burdens in the two parasite lines. Our *in vitro* binding assay showed that *P. berghei*-VAR IE adhesion to placental sections is more dependent on CSA binding than that of *P. berghei*. This observation suggests that increased *P. berghei*-VAR IE adherence is probably related to the presence of a var2CSA DBL1-6 domain, which might exhibit stronger binding properties than *P. berghei* proteins. It has been shown that less adherent strains of *P. falciparum* induced lower release of proinflammatory factors by BeWO cells (a trophoblast model) *in vitro*, suggesting that the magnitude of inflammation is associated with the affinity of IE adherence (27). Taken together, these data could explain why *P. berghei*-VAR infection results in worse pregnancy outcomes. Although var2CSA is not exposed on the surfaces of all *P. berghei*-VAR IEs, we observed a significant increase in binding to placentas and increased PM severity in *P. berghei*-VAR-infected mice compared to *P. berghei*-infected mice, indicating that var2CSA plays an important role in pathology. Further studies are needed to understand why *P. berghei*-VAR infection aggravates PM pathogenesis.

Increased susceptibility to *Plasmodium* infection in pregnant women has been well documented, but the reasons are not completely understood (28). Suppression of the immune response during pregnancy has been suggested as a risk factor. A study with Gambian women showed that the proliferative capacity of immune cells in the placenta was reduced compared to peripheral blood, which could partially explain the accumulation of parasites in the organ (29). In mouse models of PM, increased susceptibility to blood-stage infection during pregnancy is a hallmark and has been shown to occur in different mouse strains (24). Another hypothesis that could explain parasite proliferation in the peripheral blood is that IE sequestration in the placenta favors the multiplication of blood-stage parasites. It has been shown that CD36-mediated sequestration of *P. berghei* IEs favors blood-stage multiplication as a result of reduced removal of IEs from the peripheral blood circulation by the spleen (30). Evidence that could support the claim is based on our unpublished observations: the placental parasite burden greatly increased after infection and seemed to correlate with IE expansion in the maternal blood. Thus, increased sequestration in the placenta, similarly to CD36-mediated sequestration, may enhance parasite multiplication.

PM pathology is attributed to IE sequestration in the placenta, which is defined by physical interaction between var2CSA exposed on the *P. falciparum* IE membrane (11, 20) and placental cells, namely, trophoblasts. Published data support the notion that trophoblasts have an active role in the inflammatory process by reacting to IE adherence. *In vitro* studies have shown that after interaction with IEs, trophoblasts secrete interleukin 6 (IL-6) (27) and chemokines (27, 31), which in turn recruit immune cells to the site of IE stimulation (31). This inflammatory environment in the placenta can affect its anatomic structure and normal function. Thickening of the trophoblast basement membrane, which is likely to impair the normal maternal-fetal nutrient and gas exchange, has been observed in both *P. falciparum*-infected placentas (32) and *Plasmodium vivax*-infected placentas (33) and is associated with low birth weight (34). Fibrinoid necrosis was also observed in highly infected placentas (35).

In our study, IE sequestration in both the *P. berghei* and *P. berghei*-VAR PM models is likely to occur at least partially via IE adherence to CSA on trophoblasts. Evidence for this is provided by our binding assays, which show IE adherence to placentas in a CSA-dependent manner. The ability of *P. berghei* IEs to bind to CSA and to trophoblasts has been shown previously (7), and it is possible that *P. berghei* proteins exposed on the surfaces of *P. berghei* IEs bind to CSA through epitopes that share homology with DBL domains of var2CSA. Our observations that antibodies against DBL1-6 recognize *P. berghei* proteins at the IE surface support this hypothesis. Our previous observations of placentas of *P. berghei*-infected mice using intravital imaging clearly showed interaction of IEs with trophoblast areas of the placenta, where the blood flow is low; these observations and data from the current studies indicate that in the *P. berghei* PM model IEs sequester in the placenta and that placental microcirculation influences the level of IE accumulation (8). The observation that low-sulfated CS is expressed in rat placentas and binds to panselected CSA-adherent *P. falciparum* IEs *in vitro* (36) suggests that this molecule is also present in the mouse placenta and is capable of binding to var2CSA.

The use of the *P. berghei*-VAR PM model can help to clarify mechanisms underlying var2CSA-induced pathogenesis and provides a novel tool to test vaccination protocols and to understand the immune responses against var2CSA that are involved in immunological protection against PM. In fact, current questions posed by the malaria community (37), such as those concerning the effectiveness of targets to elicit protection, the function of protective antibodies, and the endurance of B cell memory and contribution of the T cell compartment, remain unanswered.

ACKNOWLEDGMENTS

We thank Jai Ramesar and Onny Klop from Leiden University Medical Center for technical support. We also thank Daniel Sobral from the Bioinformatics Unit at Instituto Gulbenkian de Ciência for assistance in data analysis.

L. V. de Moraes was supported by the FCT (fellowship SFRH/BPD/44486/2008) and the Fundação Calouste Gulbenkian de Ciência (fellowships 163/BPD/2014 and 178/BPD/2015); Chris J. Janse and Carlos Penha-Gonçalves were supported by a grant from the European Community's Seventh Framework Program (FP7/2007–2013) under grant agreement no. 242095. B. Gamain, S. Dechavanne, Anand Srivastava, B.

Franke-Fayard, and J. A. Braks were supported by the European Community's Seventh Framework Program (FP7/2007-2013; grant agreement no. 201222). Claudio R. F. Marinho was supported by Fundação de Amparo à Pesquisa do Estado de São Paulo (FAPESP) (grant no. 2014/09964-5). Flávia A. Lima and Oscar Murillo were supported by FAPESP (fellowship no. 2013/16417-8 and 2013/00981-1).

FUNDING INFORMATION

This work, including the efforts of Benoit Gamain, was funded by Seventh Framework Programme (FP7) (FP7/2007-2013 grant agreement no. 201222). This work, including the efforts of Luciana V. de Moraes, was funded by Ministry of Education and Science | Fundação para a Ciência e a Tecnologia (FCT) (EXPL IMI-IMU 0428/2013).

The funders had no role in study design, data collection and interpretation, or the decision to submit the work for publication.

REFERENCES

1. **WHO.** 2014. World malaria report 2014. WHO, Geneva, Switzerland.
2. **Ansell J, Hamilton KA, Pinder M, Walraven GEL, Lindsay SW.** 2002. Short-range attractiveness of pregnant women to Anopheles gambiae mosquitoes. Trans R Soc Trop Med Hyg **96:**113–116. http://dx.doi.org/10.1016/S0035-9203(02)90271-3.
3. **Bardají A, Sigauque B, Sanz S, Maixenchs M, Ordi J, Aponte JJ, Mabunda S, Alonso PL, Menéndez C.** 2011. Impact of malaria at the end of pregnancy on infant mortality and morbidity. J Infect Dis **203:**691–699. http://dx.doi.org/10.1093/infdis/jiq049.
4. **Nosten F, van Vugt M, Price R, Luxemburger C, Thway KL, Brockman A, McGready R, ter Kuile F, Looareesuwan S, White NJ.** 2000. Effects of artesunate-mefloquine combination on incidence of Plasmodium falciparum malaria and mefloquine resistance in western Thailand: a prospective study. Lancet **356:**297–302. http://dx.doi.org/10.1016/S0140-6736(00)02505-8.
5. **McGready R, Boel M, Rijken MJ, Ashley EA, Cho T, Moo O, Paw MK, Pimanpanarak M, Hkirijareon L, Carrara VI, Lwin KM, Phyo AP, Turner C, Chu CS, van Vugt M, Price RN, Luxemburger C, ter Kuile FO, Tan SO, Proux S, Singhasivanon P, White NJ, Nosten FH.** 2012. Effect of early detection and treatment on malaria related maternal mortality on the north-western border of Thailand 1986-2010. PLoS One **7:**e40244. http://dx.doi.org/10.1371/journal.pone.0040244.
6. **Takem EN, D'Alessandro U.** 2013. Malaria in pregnancy. Mediterr J Hematol Infect Dis **5:**e2013010. http://dx.doi.org/10.4084/MJHID.2013.010.
7. **Neres R, Marinho CR, Goncalves LA, Catarino MB, Penha-Goncalves C.** 2008. Pregnancy outcome and placenta pathology in Plasmodium berghei ANKA infected mice reproduce the pathogenesis of severe malaria in pregnant women. PLoS One **3:**e1608. http://dx.doi.org/10.1371/journal.pone.0001608.
8. **de Moraes LV, Tadokoro CE, Gómez-Conde I, Olivieri DN, Penha-Gonçalves C.** 2013. Intravital placenta imaging reveals microcirculatory dynamics impact on sequestration and phagocytosis of Plasmodium-infected erythrocytes. PLoS Pathog **9:**e1003154. http://dx.doi.org/10.1371/journal.ppat.1003154.
9. **Salanti A, Dahlbäck M, Turner L, Nielsen MA, Barfod L, Magistrado P, Jensen ATR, Lavstsen T, Ofori MF, Marsh K, Hviid L, Theander TG.** 2004. Evidence for the involvement of VAR2CSA in pregnancy-associated malaria. J Exp Med **200:**1197–1203. http://dx.doi.org/10.1084/jem.20041579.
10. **Gamain B, Trimnell AR, Scheidig C, Scherf A, Miller LH, Smith JD.** 2005. Identification of multiple chondroitin sulfate A (CSA)-binding domains in the var2CSA gene transcribed in CSA-binding parasites. J Infect Dis **191:**1010–1013. http://dx.doi.org/10.1086/428137.
11. **Duffy MF, Maier AG, Byrne TJ, Marty AJ, Elliott SR, O'Neill MT, Payne PD, Rogerson SJ, Cowman AF, Crabb BS, Brown GV.** 2006. VAR2CSA is the principal ligand for chondroitin sulfate A in two allogeneic isolates of Plasmodium falciparum. Mol Biochem Parasitol **148:**117–124. http://dx.doi.org/10.1016/j.molbiopara.2006.03.006.
12. **Fried M, Duffy PE.** 1996. Adherence of Plasmodium falciparum to chondroitin sulfate A in the human placenta. Science **272:**1502–1504. http://dx.doi.org/10.1126/science.272.5267.1502.
13. **Viebig NK, Levin E, Dechavanne S, Rogerson SJ, Gysin J, Smith JD, Scherf A, Gamain B.** 2007. Disruption of var2csa gene impairs placental malaria associated adhesion phenotype. PLoS One **2:**e910. http://dx.doi.org/10.1371/journal.pone.0000910.
14. **Tutterrow YL, Salanti A, Avril M, Smith JD, Pagano IS, Ako S, Fogako J, Leke RGF, Taylor DW.** 2012. High avidity antibodies to full-length VAR2CSA correlate with absence of placental malaria. PLoS One **7:**e40049. http://dx.doi.org/10.1371/journal.pone.0040049.
15. **Marinho CR, Neres R, Epiphanio S, Goncalves LA, Catarino MB, Penha-Goncalves C.** 2009. Recrudescent Plasmodium berghei from pregnant mice displays enhanced binding to the placenta and induces protection in multigravida. PLoS One **4:**e5630. http://dx.doi.org/10.1371/journal.pone.0005630.
16. **Baruch DI, Pasloske BL, Singh HB, Bi X, Ma XC, Feldman M, Taraschi TF, Howard RJ.** 1995. Cloning the P. falciparum gene encoding PfEMP1, a malarial variant antigen and adherence receptor on the surface of parasitized human erythrocytes. Cell **82:**77–87. http://dx.doi.org/10.1016/0092-8674(95)90054-3.
17. **Salanti A, Staalsoe T, Lavstsen T, Jensen AT, Sowa MP, Arnot DE, Hviid L, Theander TG.** 2003. Selective upregulation of a single distinctly structured var gene in chondroitin sulphate A-adhering Plasmodium falciparum involved in pregnancy-associated malaria. Mol Microbiol **49:**179–191. http://dx.doi.org/10.1046/j.1365-2958.2003.03570.x.
18. **Duffy PE, Fried M.** 2003. Antibodies that inhibit Plasmodium falciparum adhesion to chondroitin sulfate A are associated with increased birth weight and the gestational age of newborns. Infect Immun **71:**6620–6623. http://dx.doi.org/10.1128/IAI.71.11.6620-6623.2003.
19. **Pasini EM, Braks JA, Fonager J, Klop O, Aime E, Spaccapelo R, Otto TD, Berriman M, Hiss JA, Thomas AW, Mann M, Janse CJ, Kocken CHM, Franke-Fayard B.** 2013. Proteomic and genetic analyses demonstrate that Plasmodium berghei blood stages export a large and diverse repertoire of proteins. Mol Cell Proteomics **12:**426–448. http://dx.doi.org/10.1074/mcp.M112.021238.
20. **Srivastava A, Gangnard S, Round A, Dechavanne S, Juillerat A, Raynal B, Faure G, Baron B, Ramboarina S, Singh SK, Belrhali H, England P, Lewit-Bentley A, Scherf A, Bentley GA, Gamain B.** 2010. Full-length extracellular region of the var2CSA variant of PfEMP1 is required for specific, high-affinity binding to CSA. Proc Natl Acad Sci U S A **107:**4884–4889. http://dx.doi.org/10.1073/pnas.1000951107.
21. **Spaccapelo R, Janse CJ, Caterbi S, Franke-Fayard B, Bonilla JA, Syphard LM, Di Cristina M, Dottorini T, Savarino A, Cassone A, Bistoni F, Waters AP, Dame JB, Crisanti A.** 2010. Plasmepsin 4-deficient Plasmodium berghei are virulence attenuated and induce protective immunity against experimental malaria. Am J Pathol **176:**205–217. http://dx.doi.org/10.2353/ajpath.2010.090504.
22. **Janse CJ, Ramesar J, Waters AP.** 2006. High-efficiency transfection and drug selection of genetically transformed blood stages of the rodent malaria parasite Plasmodium berghei. Nat Protoc **1:**346–356. http://dx.doi.org/10.1038/nprot.2006.53.
23. **Avril M, Hathaway MJ, Srivastava A, Dechavanne S, Hommel M, Beeson JG, Smith JD, Gamain B.** 2011. Antibodies to a full-length VAR2CSA immunogen are broadly strain-transcendent but do not cross-inhibit different placental-type parasite isolates. PLoS One **6:**e16622. http://dx.doi.org/10.1371/journal.pone.0016622.
24. **Rodrigues-Duarte L, Vieira de Moraes L, Barboza R, Marinho CR, Franke-Fayard B, Janse CJ, Penha-Goncalves C.** 2012. Distinct placental malaria pathology caused by different Plasmodium berghei lines that fail to induce cerebral malaria in the C57Bl/6 mouse. Malar J **11:**231. http://dx.doi.org/10.1186/1475-2875-11-231.
25. **Muthusamy A, Achur RN, Bhavanandan VP, Fouda GG, Taylor DW, Gowda DC.** 2004. Plasmodium falciparum-infected erythrocytes adhere both in the intervillous space and on the villous surface of human placenta by binding to the low-sulfated chondroitin sulfate proteoglycan receptor. Am J Pathol **164:**2013–2025. http://dx.doi.org/10.1016/S0002-9440(10)63761-3.
26. **Clausen TM, Christoffersen S, Dahlbäck M, Langkilde AE, Jensen KE, Resende M, Agerbæk MØ, Andersen D, Berisha B, Ditlev SB, Pinto VV, Nielsen MA, Theander TG, Larsen S, Salanti A.** 2012. Structural and functional insight into how the Plasmodium falciparum VAR2CSA protein mediates binding to chondroitin sulfate A in placental malaria. J Biol Chem **287:**23332–23345. http://dx.doi.org/10.1074/jbc.M112.348839.
27. **Vásquez AM, Segura C, Blair S.** 2013. Induction of pro-inflammatory response of the placental trophoblast by Plasmodium falciparum infected

erythrocytes and TNF. Malar J **12:**421. http://dx.doi.org/10.1186/1475-2875-12-421.
28. **Menendez C.** 1995. Malaria during pregnancy: a priority area of malaria research and control. Parasitol Today **11:**178–183. http://dx.doi.org/10.1016/0169-4758(95)80151-0.
29. **Rasheed FN, Bulmer JN, Dunn DT, Menendez C, Jawla MF, Jepson A, Jakobsen PH, Greenwood BM.** 1993. Suppressed peripheral and placental blood lymphoproliferative responses in first pregnancies: relevance to malaria. Am J Trop Med Hyg **48:**154–160.
30. **Fonager J, Pasini EM, Braks JAM, Klop O, Ramesar J, Remarque EJ, Vroegrijk IOCM, van Duinen SG, Thomas AW, Khan SM, Mann M, Kocken CHM, Janse CJ, Franke-Fayard BMD.** 2012. Reduced CD36-dependent tissue sequestration of Plasmodium-infected erythrocytes is detrimental to malaria parasite growth in vivo. J Exp Med **209:**93–107. http://dx.doi.org/10.1084/jem.20110762.
31. **Lucchi NW, Peterson DS, Moore JM.** 2008. Immunologic activation of human syncytiotrophoblast by Plasmodium falciparum. Malar J **7:**42. http://dx.doi.org/10.1186/1475-2875-7-42.
32. **Galbraith RM, Fox H, Hsi B, Galbraith GM, Bray RS, Faulk WP.** 1980. The human materno-foetal relationship in malaria. II. Histological, ultrastructural and immunopathological studies of the placenta. Trans R Soc Trop Med Hyg **74:**61–72.
33. **Souza RM, Ataíde R, Dombrowski JG, Ippólito V, Aitken EH, Valle SN, Álvarez JM, Epiphânio S, Marinho CRF.** 2013. Placental histopathological changes associated with Plasmodium vivax infection during pregnancy. PLoS Negl Trop Dis **7:**e2071. http://dx.doi.org/10.1371/journal.pntd.0002071.
34. **Bulmer JN, Rasheed FN, Morrison L, Francis N, Greenwood BM.** 1993. Placental malaria. II. A semi-quantitative investigation of the pathological features. Histopathology **22:**219–225.
35. **Moshi EZ, Kaaya EE, Kitinya JN.** 1995. A histological and immunohistological study of malarial placentas. APMIS **103:**737–743. http://dx.doi.org/10.1111/j.1699-0463.1995.tb01431.x.
36. **Achur RN, Agbor-Enoh ST, Gowda DC.** 2006. Rat spongiotrophoblast-specific protein is predominantly a unique low sulfated chondroitin sulfate proteoglycan. J Biol Chem **281:**32327–32334. http://dx.doi.org/10.1074/jbc.M605841200.
37. **Kane EG, Taylor-Robinson AW.** 2011. Prospects and pitfalls of pregnancy-associated malaria vaccination based on the natural immune response to Plasmodium falciparum VAR2CSA-expressing parasites. Malar Res Treat **2011:**764845. http://dx.doi.org/10.4061/2011/764845.